DE GRUYTER

Biologia **72**/8: 869—876, 2017
Section Botany
DOI: 10.1515/biolog-2017-0104

Overexpression of Arabidopsis *ICR1* gene affects vegetative growth and anthesis

Da-Hui Li, Man-Li Li, Xiao-Bo Yu, Di Wu, Huan Xi, Yi Lin & Yong-Ping Cai*

School of Life Sciences, Anhui Agricultural University, Hefei 230036, China; e-mail: yongpcai@163.com

Abstract: Arabidopsis ICR1 (AtICR1) has been identified as a specific effector of Rho family small GTPases (ROP) in *Arabidopsis thaliana*. Previous researches have suggested that AtICR1 could function as scaffold linking ROP GTPases with vesicle trafficking and differentiation of cell polarity. To further explore whether AtICR1 is involved in potential regulation of other developmental pathways (such as anthesis), we characterized phenotypes of transgenic *Arabidopsis* ectopically expressing *AtICR1* gene in the present research. Using GST pull-down assays, a direct protein interaction between AtICR1 and AtROP2 was detected. Thereafter, subcellular localization showed that AtICR1 are transiently expressed in both cell cortex along plasma membrane and nucleus in tobacco epidermal cells. Furthermore, Transcriptional level of *AtICR1* in stable transgenic *AtICR1* lines showed 20-fold higher values compared with wild-type plants via qRT-PCR analysis. Moreover, based on the AtICR1-tagged GUS activity, it was found that the overexpression of *AtICR1* was in a constitutive pattern. Interestingly, the transgenic plants overexpressing AtICR1 exhibited dwarf and delay-for-anthesis phenotypes, as well deformed appearance of leaf epidermal cells. These results provided useful information on revealing novel roles of interactions between AtICR1 and ROP GTPases in regulation of plant development.

Key words: *Arabidopsis thaliana*; anthesis; AtICR1; overexpression; ROP GTPases.

Introduction

ROP, a plant-specific protein, is a conserved Rho family of small GTPases (Zheng & Yang 2000; Yang 2002). It is characterized as a binary switch in plant signaling: the inactive GDP-bound and the active GTP-bound states (Zheng & Yang 2000). Multiple ROPs have been found in the examined plant species, for example, at least 9 ROPs in maize, and 11 ROPs in Arabidopsis (Brembu et al. 2006). Based on phylogenetic analysis, these ROPs could be classified into four distinct groups, each with redundant and/or distinct functions (Yang 2002). ROPs play an important role in the modulation of many plant-specific signaling pathways (Craddock et al. 2012; Yang & Lavagi 2012).

Within ROP-dependent signaling pathway, they are regulated by upstream factors, then activate downstream targets via interaction with their effector proteins, such as AtICR1 (interactor of constitutive active ROPs 1) in Arabidopsis (Lavy et al. 2007; Li et al. 2008). Previous researches have revealed that AtICR1 was involved in the regulation of exocytosis through interaction with AtROP6 and AtROP10 (Lavy et al. 2007). Furthermore, the loss-of-function mutant icr1 led to small and cubical phenotypes of leaf pavement cells, whereas overexpression of AtICR1 resulted in loss of the interdigitated appearance of the pavement cells in Arabidopsis (Lavy et al. 2007). When overexpressed in Arabidopsis pollen, AtICR1 induced growth depolarization in pollen tubes, a phenotype similar to that induced by AtROP1 overexpression. It was proposed that AtICR1 was involved in the positive feedback regulation of AtROP1 localization to the plasma membrane, leading to the establishment of a polar site for pollen germination and pollen tube growth (Li et al. 2008). As small GTPases play important roles in modulating signaling pathways and functions in plants (Yang 2002), we wonder whether AtICR1 is involved in potential regulation of other developmental pathways (i.e. anthesis) beyond the known conservative functions.

In the present study, the protein-protein interaction between AtICR1 and AtROP2 was investigated by *in vitro* pull-down assay. Furthermore, we characterized phenotypes of transgenic *Arabidopsis* ectopically expressing *AtICR1* gene. These results provided the novel information on AtICR1 function in mediating small GTPase signaling in *Arabidopsis*.

Material and methods

Plant material, bacterial strains, vectors

A. thaliana plants (ecotypes Col-0) were used in the present study. Sterilized seeds were plated on 1/2 MS solid medium and kept at 4 ℃ for 3 days, then transferred to growth chambers at 22 ℃ under 16h light/ 8h dark regime. *Escherichia coli* DH5α and vector pMD18-T (TaKaRa, Japan) were used for DNA manipulation. Hosted in *E. coli* BL21 (DE3) (New

* Corresponding author

England Biolabs, USA), vector pGEX-4T-1 (General Electric Healthcare, USA) and pET-32a(+) (Novagen, USA) were used for bacterial expression of the cloned *AtICR1* and *AtROP2* gene, respectively. Plasmid pCAMBIA1304 was used to construct the chimeric gene for plant transformation.

Cloning of AtICR1 and AtROP2 cDNAs

Total RNA was isolated from ten-day-old *A. thaliana* seedlings, using an RNeasy mini kit (Qiagen, USA). Following RNA extraction, RT-PCR was performed using the protocol of RNA LA PCR^{TM} Kit (Takara, Japan). Base on the mRNA sequence of *AtICR1* (GenBank Accession No. NM_101574), a pair of primers specific to *AtICR1*, AGA TCT ATG CCA AGA CCA AGA GTT (containing a *Bgl*II site) and GGT ACC TCA CTT TTG CCC TTT CTT CCT (containing a *Kpn*I site), was designed. Similarly, another set of primers specific to *AtROP2*, GAA TTC ATG GCG TCA AGG TTT ATA AAG (containing a *EcoR*I site) and AAG CTT TCA CAA GAA CGC GCA ACG GTT (containing a *Hind*III site), was designed based on the mRNA sequence of *AtROP2* (GenBank Accession No. NM_101863). PCR products were subjected to agar electrophoresis, then the appropriate band removed and purified with a PCR Fragment Recovery Kit (Takara, Japan). The purified fragment (*AtICR1* or *AtROP2* cDNA) was then cloned into a pMD18-T vector and confirmed by DNA sequencing, respectively.

Construction of the bacterial expression vectors pGEX-AtICR1 and pET32-AtROP2

The recombinant vector pMD18-T-*AtICR1* was digested with *Bgl*II and *Kpn*I, and the resultant fragment of *AtICR1* was cloned into the *Bgl*II and *Kpn*I sites of the expression vector pGEX-4T-1, and designated as pGEX-*AtICR1*. For the recombinant vector pMD18-T-*AtROP2*, it was digested with *EcoR*I and *Hind*III, and the resultant *AtROP2* was cloned into the *EcoR*I and *Hind*III sites of the expression vector pET-32a(+), and designated as pET32-*AtROP2*. The bacterial expression vector pGEX-*AtICR1* or pET32-*AtROP2* was introduced into *E. coli* BL21 (DE3) cells by electroporation, respectively. The empty vector was also introduced into BL21 (DE3) as a negative control.

Fusion protein production in E. coli

E. coli BL21 (DE3)/pGEX-*AtICR1* or *E. coli* BL21 (DE3)/pET32-*AtROP2* were grown at 37℃ for 12 h in 5 mL LB medium containing appropriate antibiotics (100 μg ampicillin/mL). The culture was diluted 1:100 (v/v) into 300 mL of the same medium, followed by incubation at 37℃. After the cultural OD_{600} value of 0.5 was reached, isopropyl β-D-thiogalactopyranoside (IPTG) was added to each culture to a final concentration of 0.2 mM. Then, *E. coli* cells were kept on growth at 37℃ for 3 h to induce expression of fusion protein.

Purification of fusion protein AtICR1

E. coli BL21 (DE3)/ pGEX-*AtICR1* were collected by centrifugation at 5000 rpm for 10 min, and re-suspended in 100 mM phosphate buffer (pH 7.5). Then, the bacteria cell lysate was prepared by sonication at 4℃. The supernatant containing soluble target proteins was used for purification. Purification of the fusion protein AtICR1, tagged tagged with glutathione s-transferase (GST) at its N-terminus, was purified with Glutathione-Sepharose 4B (General Electric Healthcare, USA). Beads of Glutathione-Sepharose 4B loaded in a column, were pretreated by washing four times with Washing buffer (100 mM phosphate buffer, pH 7.5, 100 mM NaCl, 1 mM EDTA, 1 mM DTT), and the lysate of supernatant containing soluble GST-AtICR1 was transfer into the column, followed by washing with Elution buffer (100 mM phosphate buffer, pH 7.5, 100 mM NaCl, 10mM glutathion) without glutathion, then eluting twice with Elution buffer. The eluted target proteins were dialysed against 100 mM phosphate buffer (pH 7.5), then stored at –80℃ and ready for use.

Purification of fusion protein AtROP2

E. coli BL21 (DE3)/pET32-*AtROP2* were prepared as the above described. Purification of the fusion protein AtROP2, tagged with hexa-HIS at N-terminus, was performed with the ProBond^{TM} Purification System Kit for proteins tagged with histidines (Invitrongen, USA). The solution of the fusion protein (500 mM NaCl supplied) was mixed with 10 mL Ni-NTA agarose and loaded onto ProBond Resin column. Unbound proteins were washed away with 100 mM phosphate buffer (pH 7.5, containing 500 mM NaCl). And bound proteins were fractionally eluted out with 100 mM phosphate buffer (pH 7.5, containing 500 mM NaCl) supplemented with 150 and 250 mM imidazole, respectively. The eluted target proteins were pooled and dialysed against 100 mM phosphate buffer (pH 7.5), then stored at –80℃ until for use.

GST pull-down assay

In pull-down assays, beads bound GST-AtICR1 was mixed with HIS-AtROP2 in Binding buffer (100 mM phosphate buffer, pH 7.5, 20 mM KC1, 5 mM $MgCl_2$, 1 μM GTP GTP or GDP supplied). Another two sets of reaction systems were constructed as following: set 1 containing only HIS-AtROP2 protein as input (positive control); set 2 containing only GST-AtICR1 protein as negative control. Binding reactions were incubated at 4℃ for 2 hours. Bead-bound and unbound fractions were separated by SDS-PAGE, and transferred to nitrocellulose membranes. HIS-AtROP2 was detected with polyclonal anti-His antibody (1:1000 dilution, v/v) produced in mice (Sigma-Aldrich, USA), and using alkaline phosphatase-conjugated anti-mouse immunoglobulins (1:5000 dilution, v/v) as the secondary antibody (Sigma-Aldrich, USA). Signals were visualized by employing NBT (nitro-blue tetrazolium chloride)/BCIP (5-bromo-4-chloro-3'-indolyphosphate p-toluidine salt) in the phosphatase reaction. SDS-PAGE was performed using a 12% gel and the gel was stained with Coomassie Brilliant Blue (Sambrook et al. 1989). The concentration of proteins was determined by the Bradford method with bovine serum albumin (BSA) as standard (Bradford 1976).

Construction of plasmids containing chimeric gene for both subcellular localization of ICR1 and Arabidopsis transformation

As plasmid pCAMBIA1304 includes both reporter genes of *GFP* and *GUS*, the constructed chimeric gene would be *AtICR1-GFP-GUS* under the control of a constitutive cauliflower mosaic virus 35S (CAM35S) promoter. *AtICR1* gene was amplified by PCR using the forward primer with *Bgl*II site (5'-AGA TCT GAT GCC AAG ACC AAG AGT T-3') and reverse primer with *Spe*I (5'-ACT AGT CTT TTG CCC TTT CTT CCT-3'). The resultant fragment was cloned upstream of the *GFP* gene in a plasmid pCAMBIA1304.

Subcellular localization of ICR1protein was determined by transient expression of the constructed chimeric gene infiltrated in tobacco leaves. The GFP fluorescence images

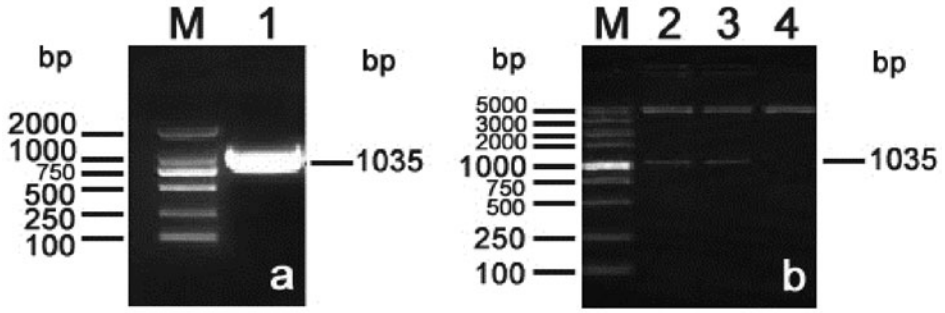

Fig. 1. Gel electrophoresis of *AtICR1* cDNA clone by RT-PCR (a) and vector pGEX-*AtICR1* by double enzymatic cutting (b). Line 1, a 1035-bp product of *AtICR1* cDNA; Lines 2 and 3, constructed pGEX-*AtICR1* with *Bgl*II-*Kpn*I cutting; Line 4, pGEX-*AtICR1* without *Bgl*II-*Kpn*I cutting as negative control; Line M, DNA mass marker.

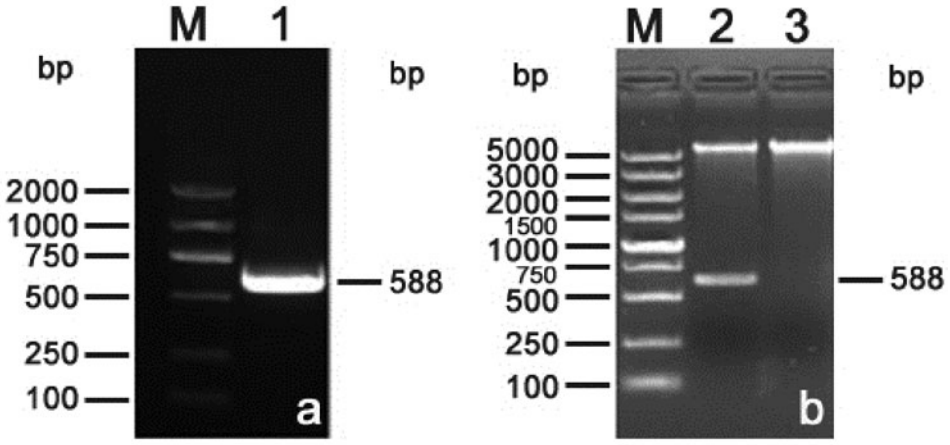

Fig. 2. Gel electrophoresis of *AtROP2* cDNA clone by RT-PCR (a) and vector pET32-*AtROP2* by double enzymatic cutting (b). Line 1, a 588-bp product of *AtROP2* cDNA; Line 2, constructed pET32-*AtROP2* with *Eco*RI-*Hind*III cutting; Line 3, pET32-*AtROP2* without *Eco*RI-*Hind*III cutting as negative control; Line M, DNA mass marker.

were collected using a confocal laser scanning microscope (Leica SP8 Confocal System, Germany).

Arabidopsis plants were transformed by the floral dip method. Kanamycin-resistant seedlings were selected and transferred to soil in pots. Plants with a single insertion were identified by segregation analysis and homozygous lines were obtained by selfing and used for further analysis. Transgenic lines were verified by *GFP* gene amplification using PCR with a pair of *GFP*-specific primers: 5'-GGA GAA GAA CTT TTC ACT GG-3' (forward) and 5'-GTA ATC CCA GCA GCT GTT AC-3' (reverse).

Real-time quantitative PCR (qPCR) analysis of AtICR1 gene expression

AtICR1-specific primer pairs: 5'-GGT GTT GAC CGT AAA TCT CCT CG-3' (forward) and 5'-AGC CAG CGG GTT TGG TTT CTT G-3' (reverse), were used for qRT-PCR analysis of *AtICR1* expression. A housekeeping gene *ACTIN* was taken as the control of transcript level. qRT-PCR was carried out using SYBR Premix Ex Taq (Takara, Japan) and ABI 7500 Real Time PCR System (Applied Biosystems, USA), with the program: 30 s at 95 °C, 40 cycles of 95 °C for 15 s, 60 °C for 20 s, 72 °C for 20 s. Normality of the cycle threshold (Ct) values of the target gene (*ICR1*) was performed based on those of endogenous reference (*actin*). Each measurement was determined through three replicates.

Histochemical staining for GUS activity

Transgenic Arabidopsis seedlings with homozygous construct of *AtICR1-GFP-GUS* were stained for GUS activity, as well the negative control from wild type Arabidopsis seedlings. The staining solution (100 mM phosphate buffer, pH 7.0, 10 mM EDTA, 0.05% Triton X-100, 0.5 mM potassium ferricyanide and potassium ferrocyanide, and 0.25 mg/mL X-glucuronide) was set for 12 h at 37 °C. After staining, seedlings were cleared in a solution of 70% (v/v) ethanol. Images were observed under the microscope (Olympus BX53, Japan) mounted with a digital camera.

Phenotype observation on plants

Arabidopsis plants were planted in pots and their phenotypes were directly observed and imaged with the digital camera (Cannon D550, Japan). For observation of epidermal cells on Arabidopsis leaves, the abaxial tissues of epidermis were manually split from the leaves, and stained with iodine solution on a glass slice, before images were taken using a microscope mounted with a digital camera.

Results

Cloning of AtICR1 cDNA

The *AtICR1* cDNA composed of 1035 bp (Fig. 1a), was cloned by RT-PCR using the specific pair of primers. Accordingly, the AtICR1 protein was deduced to possess a calculated molecular mass of 38.0 kDa. Sequencing results confirmed that *AtICR1* was consistent with the open reading frame of *AtICR1* cDNA sequence deposited in the NCBI database with GenBank Accession

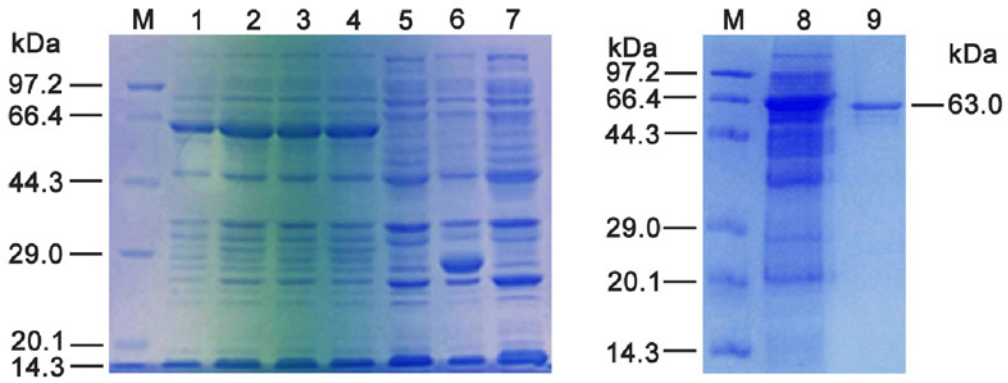

Fig. 3. SDS-PAGE analysis of the expressed protein GST-AtICR1. Lines 1-4, induced BL21/pGEX-*AtICR1*; Line 5, uninduced BL21/pGEX-*AtICR1*; Line 6, induced BL21/pGEX-4T-1; Line 7, uninduced BL21/pGEX-4T-1; Line 8, supernatant containing soluble fraction released from the induced bacteria BL21/pGEX-*AtICR1* after sonication; Line 9, purified GST-AtICR1; Line M, molecular mass marker proteins.

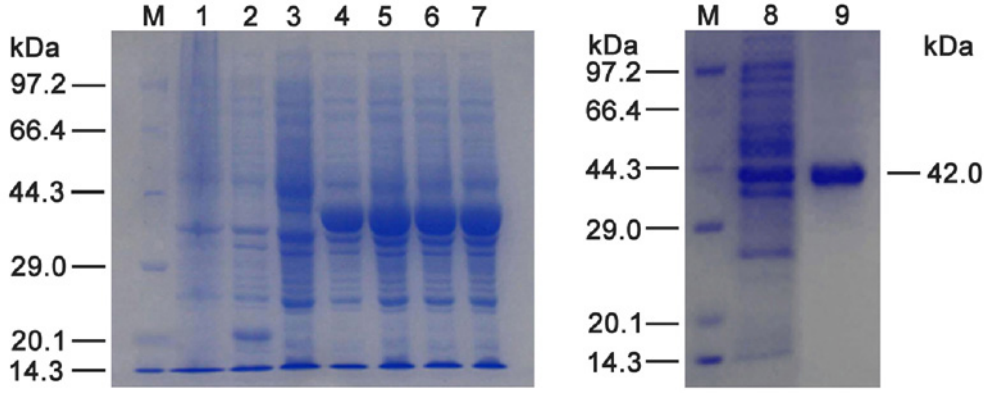

Fig. 4. SDS-PAGE analysis of the expressed protein HIS-AtROP2. Line 1, uninduced BL21/pET32-a(+); Line 2, induced BL21/pET32-a(+); Line 3, uninduced BL21/pET32-*AtROP2*; Lines 4–7, induced BL21/pET32-*AtROP2*; Line 8, supernatant containing soluble fraction released from the induced bacteria BL21/pET32-*AtROP2* after sonication; Line 9, purified HIS-AtROP2; Line M, molecular mass marker proteins.

No. NM_101574. Then the *AtICR1* cDNA was incorporated into bacterial expression vector pGEX-4T-1. The *Bgl*II and *Kpn*I digestion was used to screen the recombinant pGEX-*AtICR1* (Fig. 1b).

Cloning of AtROP2 cDNA

The *AtROP2* cDNA was cloned by RT-PCR, using the specific pair of primers to the *AtROP2* sequence deposited in the NCBI database with GenBank Accession No. NM_101863. The cloned *AtROP2* contains a 588 bp of open reading frame (Fig. 2a), which encodes a protein of 195 amino acids with a predicted molecular mass of 21.6 kDa. Then the *AtROP2* cDNA was incorporated into bacterial expression vector pET32a(+). The *EcoR*I and *Hind*III digestion was used to screen the recombinant pET32-*AtROP2* (Fig. 2b).

Bacterial expression of fusion protein AtICR1

Upon IPTG induction, the *E. coli* BL21/pGEX-*AtICR1* expressed the fusion protein GST-AtICR1 (Fig. 3, lanes 1-4), compared with the *E. coli* BL21/pGEX-4T-1 (Fig. 3, lane 6). The fusion protein consists of a 25.0 kDa of GST tag and 38.0 kDa of AtICR1. Thus the total size of the predicted fusion protein is 63.0 kDa. This roughly corresponds to the molecular size of the detected band of GST-AtICR1 on SDS-PAGE (Fig. 3). The yield of the fusion protein could reach up to 7.4% (w/w) of total BL21 proteins. Under conditions lacking IPTG induction, there was no detectable fusion protein GST-AtICR1 in the *E. coli* BL21/pGEX-*AtICR1* (Fig. 3, lane 5) and the *E. coli* BL21/pGEX-4T-1 (Fig. 3, lane 7). Furthermore, the bacteria cell lysate was centrifuged to collect the supernatant for protein purification (Fig. 3, lane 8). Through the beads Glutathione-Sepharose 4B with affinity to proteins tagged with GST, the purified fusion protein GST-AtICR1 was obtained (Fig. 3, lane 9), with a yield about 1.3 μg/mL of original bacterial culture.

Bacterial expression of fusion protein AtROP2

Upon IPTG induction, the *E. coli* BL21/pET32-*ROP2* expressed the fusion protein HIS-AtROP2 (Fig. 4, lanes 4-7), compared with the *E. coli* BL21/pET32-a(+) (Fig. 4, lane 2). The fusion protein consists of a 20.4 kDa HIS-tag and 21.6 kDa of AtROP2. Thus the total size of the predicted fusion protein is 42.0 kDa. This roughly corresponds to the molecular size of the detected band of HIS-AtROP2 on SDS-PAGE (Fig. 4).

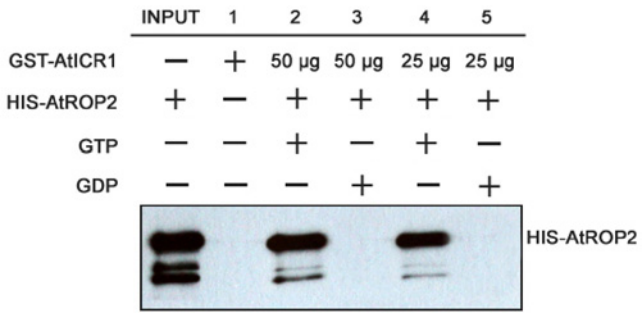

Fig. 5. *In vitro* interaction between AtICR1 and AtROP2 tested by GST pull-down assay. INPUT, using HIS-AtROP2 as positive control; Line 1, GST-AtICR1 as negative control; Lines 2 and 4, interaction between GST-AtICR1 (50 μg and 25 μg, respectively) and HIS-AtROP2 with GTP added in reaction system; Lines 3 and 5, interaction between GST-AtICR1 (50 μg and 25 μg, respectively) and HIS-AtROP2 with GDP added in reaction system; Fusion protein HIS-AtROP2, pulled down by GST-AtICR1 and probed with an anti-HIS antibody.

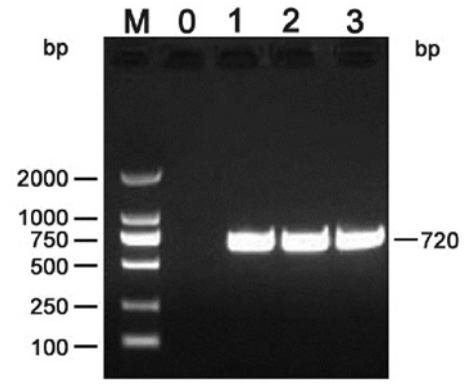

Fig. 7. Gel electrophoresis of *GFP* amplification in *Arabidopsis* plants by PCR. Line 0, wild type plants; Lines 1–3, independent *AtICR1*transgenic plants; Line M, DNA mass marker.

The yield of the fusion protein could reach up to 12.6% (w/w) of total BL21 proteins. Under conditions lacking IPTG induction, there was no detectable fusion protein HIS-AtROP2 in the *E. coli* BL21/pET32-*ROP2* (Fig. 4, lane 3) and the BL21/pET32-a(+) (Fig. 4, lane 1). Through the resin with affinity to proteins tagged with His (Fig. 4, lane 8), the fusion protein HIS-AtROP2 was purified (Fig. 4, lane 9). And the yield of the purified fusion protein was about 2.1 μg/mL of original bacterial culture.

GST pull-down assay

To test whether there is the existence of a conserved interaction between AtICR1 and AtROP2, we used the GST pull-down assay. As showed in Fig. 5, an *in vitro* protein-protein interaction was significant presented between the AtICR1 tagged with GST and the AtROP2 tagged with HIS, under the reaction condition with GTP supplied (Fig. 5). On the contrary, no interaction between AtICR1 and AtROP2 was found under the reaction condition with GDP supplied (Fig. 5). These detected bands were confirmed by corresponding ones from the input of HIS-AtROP2, whereas no*in vitro* protein-protein interaction was detected in the negative control (Fig. 5).

Subcellular localization of the AtICR1 protein

To determine ICR1 subcellular localization, transient expression was performed using AtICR1-GFP (AtICR1 fused to the green fluorescent protein) under control of the constitutive cauliflower mosaic virus 35S promoter in tobacco leaves. The AtICR1 tagged with GFP was detected in both cell cortex along plasma membrane and nucleus in tobacco epidermal cells (Fig. 6). The subcellular localization pattern suggests that AtICR1 could switch between nucleus and periphery of cytoplasm, likely due to its function in mediate the activity of ROP GTPases.

Overexpression pattern of AtICR1 in transgenic Arabidopsis

To screening stable *AtICR1* transgenic Arabidopsis, we performed PCR-based detection of *GFP* gene which was fused with *AtICR1* during the construction of plasmids for plant transformation, together with primary selection using kanamycin. As showed in Fig. 7, a 720 bp of product corresponding to GFP transcript was cloned from three independent transgenic lines using the GFP-

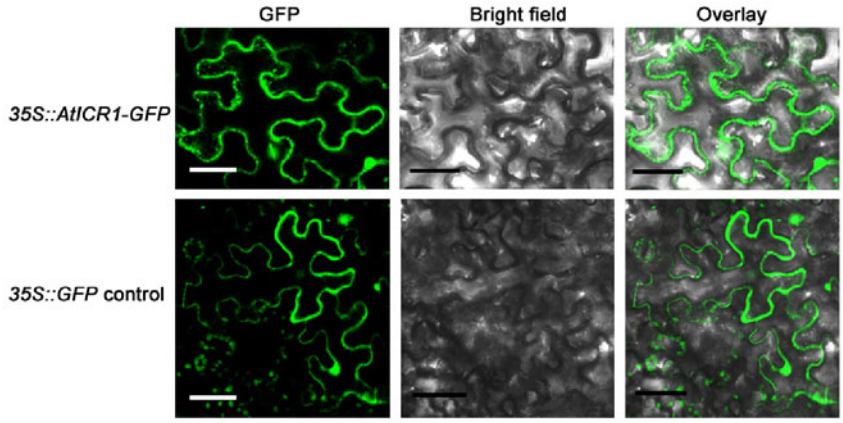

Fig. 6. Subcellular localization of AtICR1fused to GFP in tobacco epidermal cells. Bars = 50 μm.

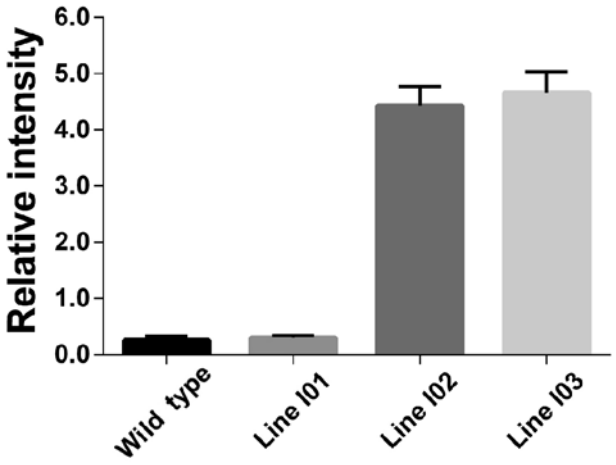

Fig. 8. qRT-PCR analysis of expression pattern of *AtICR1* in wild type and transgenic plants. Densitometic analysis gives quantitative measurements of temporal gene expression. Relative abundance of gene transcripts was determined using *ACTIN* as the internal control. The data shown are means (± standard deviation) of three experiments.

specific primer pairs. These transgenic lines were designated as Line I01, Line I02, and Line I03, and their homozygous T3 plants were used for the determination of transcription levels of *AtICR1*, respectively (Fig. 8). Two out of three transgenic lines, i.e. Line I02 and Line I03, showed significant up-regulation of *AtICR1* transcripts with a 20-fold increase on average comparing to that in the wild type Arabidopsis, using qPCR method. To further determine the overexpression pattern of *AtICR1*, we performed GUS staining for the two tested Line I02 and Line I03. One of the representative visualization of GUS signals was showed in Fig. 9. *GUS* reporter gene was expressed as a constitutive pattern throughout the whole plant (Fig. 9). Moreover *GUS* expression was enriched in both root tips and vascular tissues to a greater extent, in contrast to other parts (Fig. 9). As the constructed plasmids for the plant transformation event was under the control of the CAM35S promoter, it is feasible that the *AtICR1* overexpression should be constitutive and possess the similar transcription pattern of *GUS* reporter gene in the stable transgenic plants.

Phenotypes of the transgenic Arabidopsis overexpressing AtICR1

The transgenic plants overexpressing *AtICR1* exhibit some abnormal phenotypes with dwarf appearance to a more or less extent and the two-week or so delay for anthesis (Fig. 10a). Furthermore, overexpression of *AtICR1* resulted in the morphological change of leaf epidermal cells into more regular ones with wider necks and flatter outlines, in contrast to usually integrity of lobe and indentation appearance observed in those from the wild type Arabidopsis (Fig. 10b).

Discussion

ROP GTPases have emerged as important regulatory component in polarized cell growth, cell morphogenesis, hormone signaling, defense, and responses to oxygen deprivation (Craddock et al. 2012; Yang & Lavagi 2012). Studies on the protein-protein interaction between ROPs and their potential targets have provided some insights for revealing the regulation mechanism of ROP signaling in plant growth and development (Wu et al. 2001; Jones et al. 2002).

AtICR1 was involved in the regulation of exocytosis through interaction with AtROP6 and AtROP10 (Lavy et al. 2007). Thus, AtICR1 also act as ROP interacting protein (Lavy et al. 2007; Li et al. 2008). It has been reported that knocking down AtICR1 led to changes in both plant cells and the whole morphology (Lavy et al. 2007). These studies suggested that AtICR1 could play a bridge role in linking the GTPase ROP with downstream targets, such as vesicles transport, cellular polarity growth.

Instead of the interdigitated appearance of leaf epidermal cells in the wild type *Arabidopsis*, these cells showed more regular morphology with wider necks and flatter outlines in the transgenic lines overexpressing *AtICR1*. Our result not only reinforced the previous re-

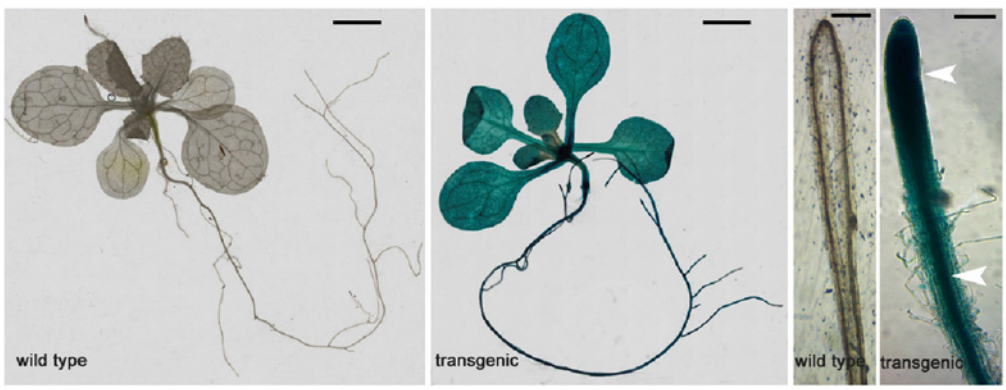

Fig. 9. *GUS* reporter gene expression in *AtICR1*transgenic plants. Wild type plants are used as negative controls. Two images at left and right sides of the panel are from whole body (bars = 2 mm) and root (bars = 0.1 mm) of plants, respectively. Arrows indicate the highly dense GUS staining in transgenic lines.

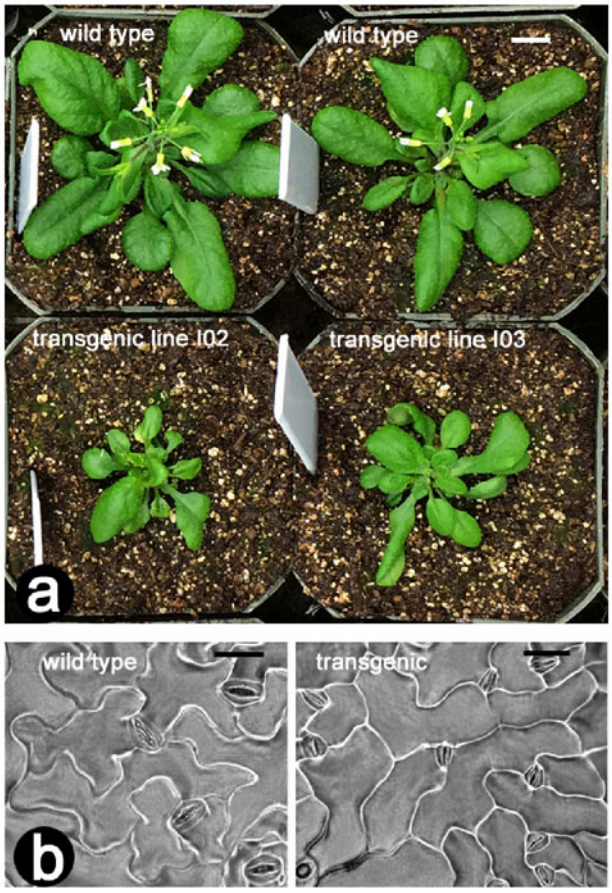

Fig. 10. Phenotypes of the transgenic *Arabidopsis* overexpressing *AtICR1*. Compared with the wild type lines (upper two pots), the transgenic ones (lower two pots) show in a status of dwarf with retarded growth and anthesis (a). Morphological images of leaf epidermal cells in wild type and transgenic plants (b). Bars = 10 mm in (a) or 10 μm in (b).

port indicating that overexpression of *AtICR1* in wild type lines could lead to morphological change in leaf epidermal cells (Lavy et al. 2007), but also implicated that the overexpressed *AtICR1* was functional in the present study. However, due to 11 AtROPs contained in *Arabidopsis*, which one of these GTPases is directly required for AtICR1 affecting cell morphogenesis remains unknown. Emerging data have firmly established that *Arabidopsis* AtROP2 could enhance the extend of lobe outgrowth of leaf epidermal cells through its interaction with two effector protein, RIC4 and RIC1, followed respectively by regulating actin microfilaments and microtubules (Fu et al. 2002; Fu et al. 2005). In our present GST pull-down assay, an interaction between AtICR1 and AtROP2 loaded with GTP was found. This result may provide the basic information on AtICR1 function in mediating AtROP2 signaling. Therefore, it is postulated that there might exist the similar ROP GTPase signaling pathway in *AtICR1* transgenic lines, analogous to wild type ones.

Furthermore, overexpression of *AtICR1* in *Arabidopsis* also resulted in dwarf phenotype, followed by delayed flowering. Despite our results which provided the novel information on AtICR1 function in mediating small GTPase signaling in *Arabidopsis*, it is still not clear in what way the overexpressed AtICR1 may be tied to these effects. Similar dwarf phenotypes were observed in the transgenic *Arabidopsis* overexpressing some *KNOX* genes, likely through affecting gibberellin biosynthesis (Tamaoki et al. 1997; Rosin et al. 2003; Yan et al. 2015). Another phytohormone, brassinosteriod (BR), may also contribute to the control of vegetative growth in plants. Loss-of-function mutation in BR biosynthetic genes, as well as the down-regulated expression of BR receptors via RNAi, resulted in dwarf phenotype in maize (Makarevitch et al. 2012; Kir et al. 2015). Next to plant hormones, transcription factors (TFs) have been implicated in many aspects of plant development. An abnormal type of growth resulted from the overexpression of specific TF genes has been observed, for example, in research of the regulation of two MYB-like genes, *MYB33* and *MYB65*. In this case when they were overexpressed in *mir159a/b* double mutants, MYB33 and MYB65 led to both the reduced leaf cell proliferation and defective pollens (Alonso-Peral et al. 2010). Plant hormones, together with transcription factors, are mainly known for their roles in regulating both of vegetative and reproductive growth. The transcription levels of *AtICR1* in transgenic lines showed 20-fold higher than those in wild type plants. Perhaps owing to such a high extent of *AtICR1* expression, the resultant AtICR1 may exert profound effects on hormone balance and/or transcription factor expression, ultimately vegetative and reproductive growth. It appears, therefore, that a considerable degree of AtICR1 level, produced by constitutive overexpression, is deleterious to plant growth.

In summary, although *AtICR1* has received the attention on its roles in leaf pavement cell formation or pollen tube growth (Lavy et al. 2007; Li et al. 2008), we observed in the present study that AtICR1 was involved in potential regulation of other developmental pathways beyond the aforementioned functions, leading to short stature and delayed flowering. Unravelling the molecular mechanism that links growth repression with AtICR1, is a task for subsequent research. Future investigation should be focused on identifying downstream genes of AtROP-AtICR1 signaling to fully understand the regulatory mechanism of our detected phenotype in transgenic *Arabidopsis* overexpressing *AtICR1*. One strategy for exploring the regulatory network is of transcriptome analysis using RNA-sequencing technology.

Acknowledgements

This work was supported by the grants from the Scientific Research Foundation for the Returned Overseas Chinese Scholars, State Education Ministry, China (No. 2015-1098), the Key University Science Research Project of Anhui Province, China (No. KJ2016A225), the Provincial Quality Engineer Fund of Anhui Education Department (No. 2015GXK015), and the Subject-Talents Program of Anhui Agricultural University (No. 2014XKPY-43).

References

Alonso-Peral M.M., Li J., Li Y., Allen R.S., Schnippenkoetter W., Ohms S., White R.G. & Millar A.A. 2010. The microRNA159-regulated GAMYB-like genes inhibit growth and promote programmed cell death in *Arabidopsis*. Plant Physiol. **154:** 757–771.

Bradford M.M. 1976. A rapid and sensitive method for the quantification of microgram quantities of protein utilizing the principle of protein-dye binding. Anal. Biochem. **72:** 248–254.

Brembu T., Winge P., Bones A.M. & Yang Z.B. 2006. A RHOse by any other name: a comparative analysis of animal and plant Rho GTPases. Cell Res. **16:** 435–445.

Craddock C., Lavagi I. & Yang Z. 2012. New insights into Rho signaling from plant ROP/Rac GTPases. Trends Cell Biol. **22:** 492–501.

Fu Y., Gu Y., Zheng Z., Wasteneys G. & Yang Z. 2005. Arabidopsis interdigitating cell growth requires two antagonistic pathways with opposing action on cell morphogenesis. Cell **120:** 687–700.

Fu Y., Li H. & Yang Z. 2002. The ROP2 GTPase controls the formation of cortical fine F-actin and the early phase of directional cell expansion during Arabidopsis organogenesis. Plant Cell **14:** 777–794.

Jones M.A., Shen J.J., Fu Y., Li H. & Yang Z.B. 2002. The Arabidopsis ROP2 GTPase is a positive regulator of both root hair initiation and tip growth. Plant Cell **14:** 763–776.

Kir G., Ye H., Nelissen H., Neelakandan A.K., Kusnandar A.S., Luo A., Inze D., Sylvester A.W., Yin Y. & Becraft P.W. 2015. RNA interference knockdown of BRASSINOSTEROID INSENSITIVE1 in maize reveals novel functions for brassinosteroid signaling in controlling plant architecture. Plant Physiol. **169:** 826–839.

Lavy M., Bloch D., Hazak O., Gutman I., Poraty L., Sorek N., Sternberg H. & Yalovsky H. 2007. A novel ROP/RAC effector links cell polarity, root-meristem maintenance, and vesicle trafficking. Cur. Biol. **17:** 947–952.

Li S.D., Gu Y., Yan A., Lord E. & Yang Z.B. 2008. RIP1 (ROP Interactive Partner1)/ICR1 marks pollen germination sites and may act in the ROP1 pathway in the control of polarized pollen growth. Mol. Plant **1:** 1021–1035.

Makarevitch I., Thompson A., Muehlbauer G.J. & Springer N.M. 2012. *Brd1* gene in maize encodes a brassinosteroid C-6 oxidase. PLoS ONE **7:** e30798.

Rosin F.M., Hart J.K., Horner H.T., Davies P.J. & Hannapel D.J. 2003. Overexpression of a knotted-like homeobox gene of potato alters vegetative development by decreasing gibberellin accumulation. Plant Physiol. **132:** 106–117.

Sambrook J., Fritsch E.F. & Maniatis T. 1989. Molecular cloning. Cold Spring Harbor, New York.

Tamaoki M., Kusaba S., Kano-Murakami Y. & Matsuoka M. 1997. Ectopic expression of a tobacco homeobox gene, *NTH15*, dramatically alters leaf morphology and hormone levels in transgenic tobacco. Plant Cell Physiol. **38:** 917–927.

Wu G., Gu Y., Li S. & Yang Z.B. 2001. A genome-wide analysis of Arabidopsis Rop-interactive CRIB motif-containing proteins that act as Rop GTPase targets. Plant Cell **13:** 2841–2856.

Yan F., Hu G.J., Ren Z.X., Deng W. & Li Z.G. 2015. Ectopic expression a tomato KNOX Gene *Tkn4* affects the formation and the differentiation of meristems and vasculature. Plant Mol. Biol. **89:** 589–605.

Yang Z.B. 2002. Small GTPase: versatile signaling switches in plant. Plant Cell **14 (Suppl.):** S375–S388.

Yang Z.B. & Lavagi I. 2012. Spatial control of plasma membrane domains: ROP GTPase-based symmetry breaking. Curr. Opin. Plant Biol. **15:** 601–607.

Zheng Z.L. & Yang Z.B. 2000. The Rop GTPase: an emerging signaling switch in plants. Plant Mol. Biol. **44:** 19.

Received January 10, 2017
Accepted April 26, 2017